

Assembly of the Herpes Simplex Virus Capsid: Identification of Soluble Scaffold-Portal Complexes and Their Role in Formation of Portal-Containing Capsids

William W. Newcomb,¹ Darrell R. Thomsen,² Fred L. Homa,² and Jay C. Brown^{1*}

Department of Microbiology and Cancer Center, University of Virginia Health System, Charlottesville, Virginia 22908,¹ and Infectious Disease Research, Pharmacia Corporation, Kalamazoo, Michigan 49001²

Received 17 April 2003/Accepted 18 June 2003

The herpes simplex virus type 1 (HSV-1) portal complex is a ring-shaped structure located at a single vertex in the viral capsid. Composed of 12 U_L6 protein molecules, the portal functions as a channel through which DNA passes as it enters the capsid. The studies described here were undertaken to clarify how the portal becomes incorporated as the capsid is assembled. We tested the idea that an intact portal may be donated to the growing capsid by way of a complex with the major scaffolding protein, U_L26.5. Soluble U_L26.5-portal complexes were found to assemble when purified portals were mixed *in vitro* with U_L26.5. The complexes, called scaffold-portal particles, were stable during purification by agarose gel electrophoresis or sucrose density gradient ultracentrifugation. Examination of the scaffold-portal particles by electron microscopy showed that they resemble the 50- to 60-nm-diameter “scaffold particles” formed from purified U_L26.5. They differed, however, in that intact portals were observed on the surface. Analysis of the protein composition by sodium dodecyl sulfate-polyacrylamide gel electrophoresis demonstrated that portals and U_L26.5 combine in various proportions, with the highest observed U_L6 content corresponding to two or three portals per scaffold particle. Association between the portal and U_L26.5 was antagonized by WAY-150138, a small-molecule inhibitor of HSV-1 replication. Soluble scaffold-portal particles were found to function in an *in vitro* capsid assembly system that also contained the major capsid (VP5) and triplex (VP19C and VP23) proteins. Capsids that formed in this system had the structure and protein composition expected of mature HSV-1 capsids, including U_L6, at a level corresponding to ~1 portal complex per capsid. The results support the view that U_L6 becomes incorporated into nascent HSV-1 capsids by way of a complex with U_L26.5 and suggest further that U_L6 may be introduced into the growing capsid as an intact portal.

All herpesviruses have the same basic structure, a rigid icosahedral capsid surrounded by a membrane envelope. The capsid contains the virus DNA in a highly condensed form in which it is protected from mechanical and other damage. The capsid also functions to release the viral DNA into the host cell nucleus shortly after a new cycle of infection is initiated (33, 34).

The structure of the herpes simplex virus type 1 (HSV-1) capsid has been studied extensively and was found to be similar to that of other herpesviruses (38, 44, 49). Composed entirely of protein, the HSV-1 capsid is an icosahedral shell ~125 nm in diameter and 15 nm thick. Its major structural features are 162 capsomers (150 hexons and 12 pentons) that lie on a T = 16 icosahedral lattice. The hexons are found on the capsid edges and faces, while the pentons are located at the vertices. The capsomers are connected in groups of three by the triplexes, trivalent structures composed of U_L18 and U_L38 that lie above the capsid floor.

The 150 hexons resemble each other in that all have the same protein composition, six molecules of U_L19 (the major capsid protein, VP5) and six of U_L35 (VP26 [33, 38]). The pentons, however, are of two different compositions. Eleven of

the 12 are pentamers of U_L19, while the 12th, the unique vertex, is a cylindrical structure called the portal (27). The portal is composed of 12 U_L6 molecules and has an axial channel through which DNA is introduced into the capsid. The portal is thought to play an active role in DNA encapsidation, but its precise mechanism of action has not yet been defined (30, 36, 37, 39).

The basic features of the HSV-1 capsid assembly pathway have now been identified in studies carried out both *in vivo* and *in vitro* (3, 10, 24, 25, 26, 38, 40, 42). Assembly is found to require the components of the capsid shell (U_L19, U_L35, U_L18, and U_L38) and also the scaffolding protein, U_L26.5. The scaffolding protein participates in capsid formation, but thereafter it is lost and is not found in the mature capsid or virion. Capsid assembly proceeds by way of small oligomers containing one or a few molecules each of the major capsid and scaffolding proteins. These presumably add to the edges of the growing capsid and are secured in place by the triplexes. The nascent capsid eventually closes, forming the procapsid, a spherical structure with approximately the same diameter as the capsid (24, 29, 43). The procapsid matures by way of a structural transformation to create the mature capsid (9). The scaffolding protein is lost, possibly as DNA enters and the procapsid matures.

Although important information about capsid assembly is now available, as described above, it is not yet clear how the portal complex becomes incorporated into the growing structure. It is possible, in fact, that quite subtle interactions may be

* Corresponding author. Mailing address: Department of Microbiology, Box 800734, University of Virginia Health System, 1300 Jefferson Park Ave., Charlottesville, VA 22908. Phone: (434) 924-1814. Fax: (434) 982-1071. E-mail: JCB2G@virginia.edu.

involved, as the portal must be assembled into 1, and only 1, of the 12 geometrically identical capsid vertices.

In attempting to determine how the portal is incorporated, we have tested the idea that it is donated to the growing capsid from a complex with the scaffolding protein. It is reasonable to think this might be the case because the major capsid protein is also considered to be added to the growing shell in a complex with the scaffold (11, 16, 25, 41). In testing the proposed role of U_L26.5, we observed that soluble U_L26.5-portal complexes can form *in vitro*, and here we describe some of the properties of the complexes. The complexes were also tested in an *in vitro* capsid assembly system to determine whether they can serve as a source of the portal complex as the capsid is assembled.

MATERIALS AND METHODS

Protein purification. U_L6, U_L26.5, VP22a (U_L26.5/304), U_L26/61, and VP5 (U_L19) proteins were purified from insect cells expressing them after single infection with an appropriate recombinant baculovirus (rBV). Similarly, triplexes were purified from insect cells coinfecting with rBV encoding VP19C (U_L38) and VP23 (U_L18). The creation of the seven rBVs, BAC-U_L6, BAC-U_L26.5, BAC-U_L26.5/304, BAC-U_L26/61, BAC-U_L19, BAC-U_L38, and BAC-U_L18, was described previously (18, 41, 42). BAC-U_L26.5/304 encodes VP22a, a truncated form of U_L26.5 lacking the C-terminal 25 amino acids required for interaction of U_L26.5 with the major capsid protein (VP5) (12). U_L26/61 encodes an enzymatically inactive mutant of the protease in which His61 is changed to glutamine (41). Previously described procedures were employed for the infection of *Spo-doptera frugiperda* (Sf9) cells with rBV (multiplicity of infection, 5) and for the incubation of infected cells at 28°C for 64 h (27, 42). After incubation at 28°C, the infected cells were centrifuged into a pellet, frozen in 5-ml aliquots, thawed, resuspended in 10 ml of phosphate-buffered saline (PBS) containing 1.5 ml of a protease inhibitor cocktail (prepared by dissolving one tablet of Boehringer Mannheim Complete EDTA-free in 5 ml of PBS), and frozen in 1-ml aliquots. The 1-ml aliquots were used for all subsequent steps of protein purification. U_L6 was purified by the previously described method (27), which yields intact portals in 20 mM Tris-HCl, pH 7.5, containing 1 M arginine and ~20% sucrose. The protein concentrations of individual U_L6 preparations varied, but all were in the range of 0.2 to 0.4 mg/ml.

U_L26.5 was prepared by a modification of a procedure described previously (17, 25). All purification steps were carried out at 4°C. A 1-ml aliquot of frozen, rBV-infected cells (as described above) was thawed quickly, and the lysate was clarified by centrifugation for 5 min at 16,000 × g. The supernatant (clarified lysate) was added to 0.2 volume of saturated ammonium sulfate, incubated for 10 min at 4°C, and centrifuged for 5 min at 16,000 × g to collect the precipitate, which contained U_L26.5. The precipitate was suspended in 400 μl of PBS containing 2 mM EDTA, 5 mM dithiothreitol (DTT), and 40 μl of protease inhibitor cocktail (see above) and incubated overnight at 4°C to solubilize U_L26.5. The resulting cloudy suspension was centrifuged at 16,000 × g for 15 min, and the supernatant was used as a source of U_L26.5 in the experiments described below. The U_L26.5 protein concentration was in the range of 1 to 2 mg/ml, and the preparations were used promptly (the same day) without refreezing. The same procedure was employed for purification of U_L26.5-U_L6 complexes and U_L26/61.

VP22a was purified from BAC-U_L26.5/304-infected insect cells by the same procedure described above for U_L26.5 except that DTT was omitted from the solution used to solubilize the ammonium sulfate precipitate. VP5 and triplexes (heterotrimers containing one VP19C and two VP23 molecules) were purified by a method described previously (23). For use in capsid assembly reactions, VP5 and triplexes were dissolved in PBS containing 10 mM EDTA.

U_L26.5-U_L6 complex formation *in vitro*. Complexes were assembled by mixing U_L26.5 and U_L6 solutions and incubating the mixture. In a typical experiment, 10 μl of U_L26.5 (~15 μg or 440 pmol of protein) was mixed with 10 μl of PBS plus 2 μl of U_L6 (~0.6 μg or 8 pmol) and incubated for 15 min at room temperature. The solution was then centrifuged for 2 min at 16,000 × g, and the supernatant was used as described below for agarose gel electrophoresis, sucrose density gradient ultracentrifugation, electron microscopy, or capsid assembly. In reactions used to test the effect of WAY-150138 on complex formation, the drug (2 μl, with the concentration adjusted to achieve the desired concentration in the reaction mixture) was added in dimethyl sulfoxide solvent, and U_L6 was the last component added to the reaction mixtures.

Agarose gel electrophoresis and sucrose gradient analyses. Electrophoresis of U_L26.5-U_L6 complexes and related materials was carried out with 15-μl specimens that contained 2 μl of 15% Ficoll-0.25% bromophenol blue dye. Gels of 1% agarose were 8 cm long, 6 cm wide, and 5 mm thick; they were prepared and run in 20 mM Tris-phosphate, pH 7.5. The specimens were electrophoresed at 80 to 100 V for 80 to 90 min (until 10 min after the bromophenol blue dye migrated off the gel). After electrophoresis, the gel was blotted electrophoretically onto a nitrocellulose sheet in a Hoefer TE series chamber for 90 min at 100 mA in 20 mM Tris-phosphate, pH 7.5. To visualize protein bands, the nitrocellulose sheet was stained for 5 min with 0.1% Ponceau S (FisherBiotech) in 1% acetic acid, and the results were recorded by densitometric scanning as described previously (22, 29). The sheet was then destained in water and used for staining with specific antibodies as described below. Sucrose gradient analysis was performed with 50-μl specimens which were sedimented on 0.7-ml gradients of 10 to 30% sucrose containing PBS and prepared in 5- by 41-mm tubes. The gradients were centrifuged for 2 h at 24,000 rpm in a Beckman SW 50.1 rotor maintained at 4°C. After centrifugation, the gradients were separated into 13 fractions by bottom puncture of the tube, and the fractions were analyzed by sodium dodecyl sulfate (SDS)-polyacrylamide gel electrophoresis or electron microscopy as described below.

***In vitro* capsid assembly.** Assembly reaction mixtures contained 250 μl of U_L19 (VP5; 0.9 mg/ml), 250 μl of triplexes (U_L18 and U_L38; 1.2 mg/ml), 500 μl of U_L26.5-U_L6 complexes (~1 mg/ml; prepared from insect cells coinfecting with BAC-U_L6 and BAC-U_L26.5 or from U_L26.5-U_L6 particles formed *in vitro*), and 50 μl of U_L26/61 (~1 mg/ml). After the four components were mixed, the solution was adjusted to 2 mM EDTA, 5 mM DTT, and protease inhibitor cocktail (0.1 volume; see above) was added. The solution was then incubated at 32°C for 8 h to allow capsids to form. To isolate the capsids, the reaction mixtures were centrifuged briefly (1 min at 16,000 × g) to remove insoluble material, diluted to 5 ml with TNE (20 mM Tris-HCl [pH 7.5], 0.5 M NaCl, 1 mM EDTA), added to an SW 50.1 tube containing a 0.5-ml "cushion" of 35% sucrose in TNE, and centrifuged for 1 h at 23,000 rpm. The capsids, which are found in the sucrose cushion, were added to 0.5 ml of TNE, disaggregated by brief sonication, and purified by centrifugation on a 5-ml gradient of 20 to 50% sucrose prepared in TNE. The gradient was centrifuged at 23,000 rpm for 1 h in an SW50.1 rotor at 4°C. After centrifugation, the gradients were photographed (with top illumination) to record the positions of capsid bands. The capsids were then removed with a Pasteur pipette, diluted to 5 ml with TNE, sedimented into a pellet by centrifugation for 1 h at 23,000 rpm in an SW50.1 rotor, and purified by a second step of sucrose gradient centrifugation (described below) either before or after treatment with 2.0 M guanidine-HCl (GuHCl). The capsids to be treated with GuHCl were suspended in 400 μl of TNE, mixed with 200 μl of 6.0 M GuHCl, incubated for 15 min at 4°C, and centrifuged into a pellet in an SW50.1 rotor as described above. The second step of sucrose gradient purification was carried out with pelleted capsids (either before or after GuHCl treatment). These were suspended in 50 μl of TNE and centrifuged on a 0.7-ml gradient of 20 to 50% sucrose for 45 min at 23,000 rpm in an SW50.1 rotor. The gradient was then fractionated by bottom puncture of the tube, and the fractions were analyzed by electron microscopy, SDS-polyacrylamide gel electrophoresis, and Western immunoblotting for U_L6 protein as described below.

Other methods. Previously described procedures were used for SDS-polyacrylamide gel electrophoresis, staining of gels with Coomassie blue, and quantitation of bands by densitometric scanning (22, 29). Procedures described by Newcomb et al. (29) were employed for Western immunoblotting and for staining of blots with monoclonal antibody 1C9 specific for U_L6 (see below), which was used at a dilution of 1:10,000. The amounts of U_L6 present in capsids assembled *in vitro* were determined, beginning with densitometric scans of U_L6 immunoblots. The integrated density of U_L6 staining was divided by the amount of VP5 (which was taken as a measure of the total number of capsids) present in the same gel lane. The U_L6/VP5 ratio was scaled by determining the same ratio for B capsids (isolated from Vero cells infected with HSV-1) determined in the same electrophoretic gel and assumed to correspond to 12 U_L6 monomers per capsid. The amount of VP5 was determined by densitometric scanning of the blot after Ponceau S staining as described above or by Coomassie staining of a sister gel. Electron microscopy was performed with specimens that were adsorbed to carbon-Formvar-coated grids, stained for 1 min with 1% uranyl acetate, air dried, and photographed in a Philips 400T electron microscope operated at 80 keV. The images were digitized and measured with Photoshop version 5.0 as previously described (27).

U_L6-specific mouse monoclonal antibody 1C9. Hybridoma cell lines secreting U_L6-specific antibodies were isolated, beginning with spleen cells prepared from immunized mice. Four female BALB/c mice (10 weeks old) were immunized with 50 μg of purified U_L6 on two occasions separated by 4 weeks. After a further

4 weeks, one mouse was injected intrasplenically with 50 μ g of U_L6. Spleen cells were harvested 4 days later and fused with Sp2/O-Ag14 myeloma cells (35). Hybridoma cells were then selected and cloned from the fused population. The clones were tested for U_L6-specific antibody production by enzyme-linked immunosorbent assay using purified U_L6 protein as an antigen (5, 27). Clone 1C9 was subcloned and expanded by growth in vitro. Antibody was purified from the culture supernatant by adsorption and elution from protein G-Sepharose (6). The purified antibody (0.9 mg/ml; immunoglobulin G1 subclass) was found to recognize purified U_L6 in enzyme-linked immunosorbent assays and Western immunoblot tests.

RESULTS

U_L26.5-U_L6 complex formation. The ability of U_L26.5 and U_L6 to interact was tested by mixing purified U_L6 with U_L26.5 and using agarose gel electrophoresis to analyze the mixture for the presence of soluble complexes. U_L26.5 was purified in the form of 55-nm-diameter scaffold particles (17, 25), while U_L6 was solubilized in buffer containing 1 M arginine, yielding a preparation of intact portals as described previously (27). Mixing U_L6 with U_L26.5 was done under conditions in which the U_L6 arginine concentration was diluted to a level (~0.1 M) at which U_L6 precipitates (27); U_L6 could remain in solution only by forming a complex with U_L26.5. Experiments were performed by mixing the reaction components, incubating them, and centrifuging them briefly to remove any insoluble U_L6. The soluble fraction was then analyzed for U_L26.5-U_L6 complexes by agarose gel electrophoresis followed by Western immunoblotting.

The results demonstrated that U_L6 comigrated during electrophoresis with U_L26.5 scaffold particles as shown in Fig. 1a, lane 2. As expected, no soluble U_L6 was observed in reaction mixtures lacking U_L26.5, as shown in Fig. 1a, lane 3. We interpret the comigration of U_L6 and U_L26.5 to indicate the formation of a soluble complex between the two proteins. The ability of U_L26.5 and U_L6 to form soluble complexes was not affected by substantial (at least 10-fold) changes in the concentration of either reaction component, by incubating the reaction mixtures at 37°C rather than at room temperature, or by incubating them for 3 h rather than 15 min (data not shown). Using the same experimental design, U_L6 was found to form soluble complexes with VP22a, a U_L26.5 deletion lacking the C-terminal 25 amino acids (Fig. 1a, lane 5). Portal binding to VP22a indicates that the C-terminal 25 amino acids of U_L26.5 are dispensable for binding to U_L6. In contrast, no binding of U_L6 was observed with the control proteins bovine serum albumin (Fig. 1b) and DNase I (data not shown).

Agarose gels showed a variable amount of U_L6-containing material migrating more slowly than the predominant scaffold particle species (Fig. 1b, rightmost lane). When present, this region stained strongly for U_L6 but very weakly for U_L26.5 (Fig. 1b). We interpret this broad region to indicate the presence of a population of soluble U_L26.5-U_L6 complexes containing primarily U_L6 with a relatively small amount of U_L26.5.

The amount of U_L6 bound to scaffold particles was determined quantitatively, beginning with reaction mixtures in which a fixed amount of U_L26.5 was added to different amounts of U_L6. Complexes were then isolated by sucrose density gradient centrifugation, and individual gradient fractions were analyzed by SDS-polyacrylamide gel electrophoresis and staining with Coomassie blue, as shown in Fig. 2a. The amounts of U_L26.5 and U_L6 were determined quantitatively by

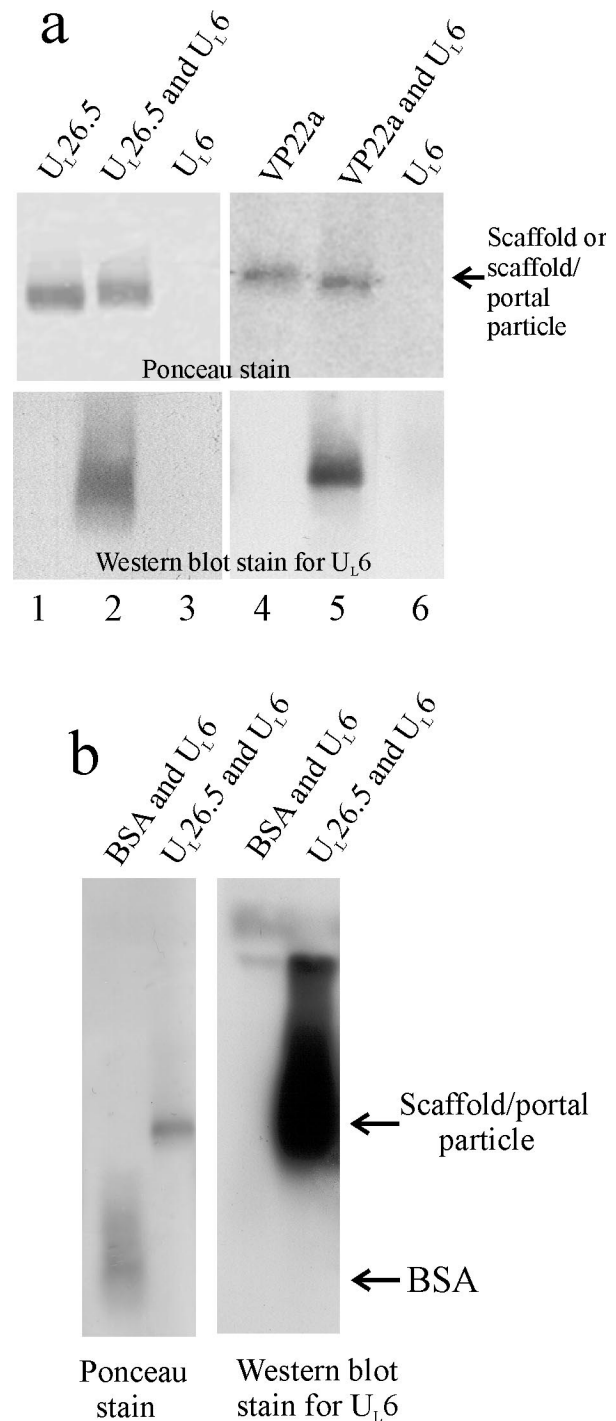


FIG. 1. Agarose gel electrophoresis of complexes containing the portal (U_L6). Reaction components were mixed and subjected to electrophoresis as described in Materials and Methods. The gel was then blotted electrophoretically onto nitrocellulose paper, which was stained with Ponceau S, destained, and stained with antibody specific for U_L6. (a) Note that U_L6 is soluble in the presence of U_L26.5 or VP22a. (b) Note that U_L6 is solubilized by U_L26.5 but not by bovine serum albumin (BSA).

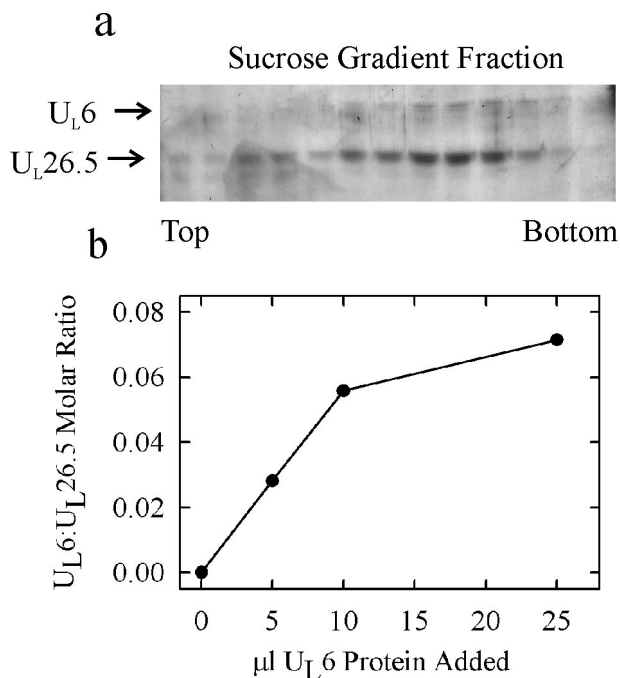


FIG. 2. Determination of the $U_L6/U_L26.5$ ratio in scaffold-portal particles. Scaffold-portal particles formed in vitro with different amounts of U_L6 were isolated by sedimentation on sucrose density gradients as described in Materials and Methods. The gradient fractions were then analyzed by SDS-polyacrylamide gel electrophoresis (a), followed by densitometric scanning of the stained gel. The gels were all similar to the one shown in panel a, where $7.5 \mu\text{g}$ of U_L6 was mixed with $38 \mu\text{g}$ of $U_L26.5$. (a) Note that U_L6 and $U_L26.5$ migrated coincidentally during centrifugation, suggesting they are part of the same complex. (b) The $U_L6/U_L26.5$ ratio in scaffold-portal particles was determined by summing the U_L6 and $U_L26.5$ amounts over all positive fractions, and the $U_L6/U_L26.5$ ratio was plotted as a function of the input U_L6 amount. Note the nonlinear binding of U_L6 at a high input U_L6 concentration.

densitometric scanning of the stained gel and summing among positive fractions.

The results demonstrated that U_L6 cosedimented with $U_L26.5$ during sucrose gradient centrifugation (Fig. 2a), suggesting the formation of a complex between the two proteins, as expected from the agarose gel observations described above. Quantitative measurements demonstrated greater U_L6 binding when more U_L6 was added to the reaction mixtures (Fig. 2b). All U_L6 added was found to be associated with scaffold particles at the lowest U_L6 amounts tested (i.e., $5 \mu\text{l}$ or $\sim 1.5 \mu\text{g}$ and $10 \mu\text{l}$ or $\sim 3 \mu\text{g}$ of U_L6 added to $\sim 38 \mu\text{g}$ of scaffold particles). At the highest U_L6 level tested ($7.5 \mu\text{g}$), however, not all added U_L6 was bound, suggesting nonlinearity in U_L6 binding. The largest observed amount of bound U_L6 corresponded to a $U_L6/U_L26.5$ molar ratio of ~ 0.07 , or $\sim 14 U_L26.5$ molecules for each U_L6 molecule.

Electron microscopy of $U_L26.5$ - U_L6 complexes. Electron microscopic analysis of scaffold and scaffold-portal particles was performed with specimens prepared in vitro by mixing scaffold particles with solvent (control) or U_L6 followed by sucrose gradient centrifugation. Samples of the peak fractions were examined after negative staining. Images of scaffold particles

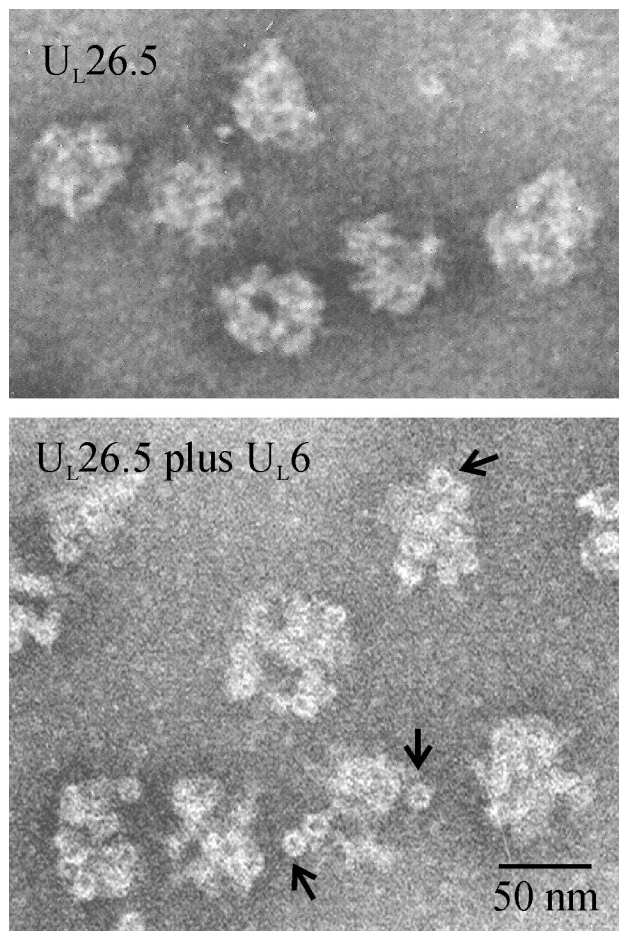


FIG. 3. Electron microscopic analysis of scaffold particles (top) and scaffold-portal particles (bottom). Note the presence of intact portals (arrows) in scaffold-portal particles.

(Fig. 3, top) showed that they were heterogeneous in both size and shape, as reported by McClelland et al. (17). The observed heterogeneity appeared to result from real differences in particle structure rather than from different views of an invariant structure. The differences in particle size, for example, suggest authentic heterogeneity among the particles. Within individual particles, the protein appeared to be densely concentrated in some areas and relatively depleted in others with no regular geometric pattern relating them.

Images of scaffold-portal particles were similar to those of scaffold particles except that small, uniformly sized rings were seen, often at the periphery of the overall structure (Fig. 3, bottom). No rings were visible in many particles, but in others, one to four rings could be seen. Measurement of the ring diameter yielded $16.2 \pm 1.9 \text{ nm}$ ($n = 51$), a value in satisfactory agreement with the reported diameter of the portal (16.4 nm [27]). We interpret the rings to be intact portals because they were seen in scaffold-portal, but not in scaffold-only, particles and because their diameter is similar to that of isolated portals. Images of scaffold-portal particles formed in vitro (Fig. 3, bottom) were the same as those obtained with scaffold-portal particles isolated from insect cells coinfecting with $U_L26.5$ and U_L6 (data not shown).

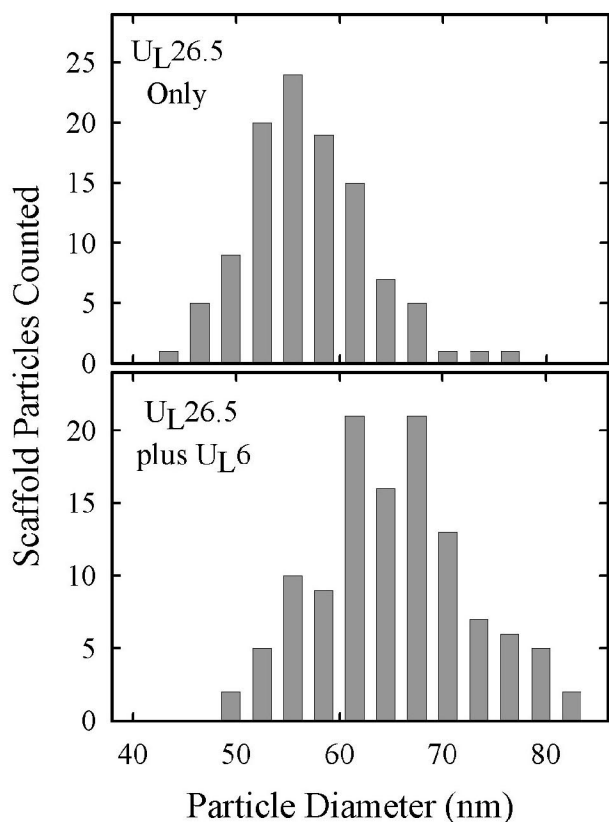


FIG. 4. Histograms showing the diameters of scaffold particles (top) and scaffold-portal particles (bottom) as measured from electron micrographs such as those shown in Fig. 3. The largest dimension across the particle was considered the diameter, as described in Materials and Methods. Note that the particle diameter is larger in scaffold-portal (bottom) than in scaffold (top) particles.

Scaffold and scaffold-portal particles were characterized by measuring the longest dimension across the particle image. The average “diameter” measured in this way was found to be 56.9 ± 5.5 nm ($n = 108$) and 64.7 ± 6.9 nm ($n = 117$) for scaffold and scaffold-portal particles, respectively. The distribution of measurements suggested a single population of particles in the case of scaffold particles (Fig. 4, top) but a greater degree of heterogeneity in scaffold-portal particles (Fig. 4, bottom). For example, particles with diameters of 70 to 80 nm may constitute a distinct population.

Effect of WAY-150138. The effect of WAY-150138 on $U_L26.5$ - U_L6 complex formation was examined to test the idea that inhibition of this association may be part of the way the drug antagonizes HSV-1 replication in cell culture (23, 47). Experiments were carried out by mixing purified scaffold particles with portals in the presence of WAY-150138 or a solvent control. The extent of U_L6 binding was then determined by agarose gel electrophoresis followed by Western immunoblotting as described above.

The results showed that the drug caused a decrease in the amount of U_L6 bound, with the maximum inhibition in the range of three- to fourfold (Fig. 5). Fifty percent inhibition of binding was observed at ~ 2.5 μ g of WAY-150138/ml, a concentration that produces a substantial ($>50\%$) reduction in

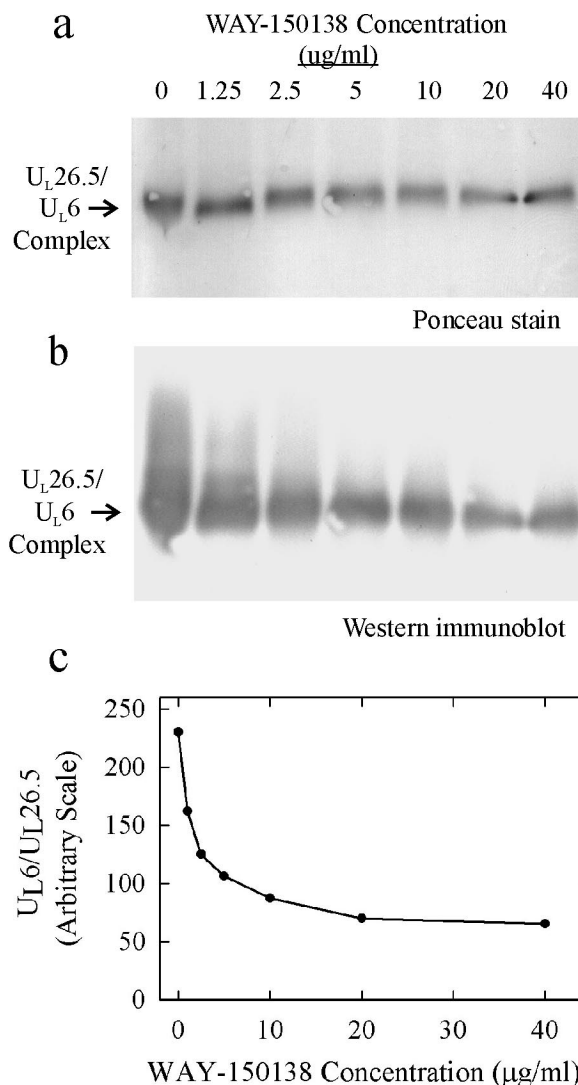


FIG. 5. Effect of WAY-150138 on formation of scaffold-portal particles in vitro. Portals and scaffold particles were mixed in vitro in the presence of WAY-150138 and subjected to electrophoresis on an agarose gel. The gel was then blotted electrophoretically onto nitrocellulose paper, which was stained with Ponceau S (a), destained, and stained with antibody specific for U_L6 (b). The amount of U_L6 binding was then determined by densitometric scanning of the U_L6 -stained bands, with a correction applied to account for small differences in the amount of $U_L26.5$ present (c). Note that the amount of U_L6 bound to scaffold particles decreased with increasing WAY-150138 concentration.

HSV-1 replication (Fig. 5c) (47). The decrease in the amount of bound U_L6 did not affect the rate at which scaffold particles migrated during agarose gel electrophoresis (Fig. 5a, and b); scaffold-portal particles from control and inhibited reactions had the same mobility.

In vitro capsid assembly. An in vitro capsid assembly system was used to determine whether scaffold-portal particles could serve as a source of portals as capsids are formed. The system was constituted by mixing scaffold-portal particles with purified major capsid protein (VP5), triplexes, and $U_L26/61$. After being mixed, the reaction components were incubated for 8 h at

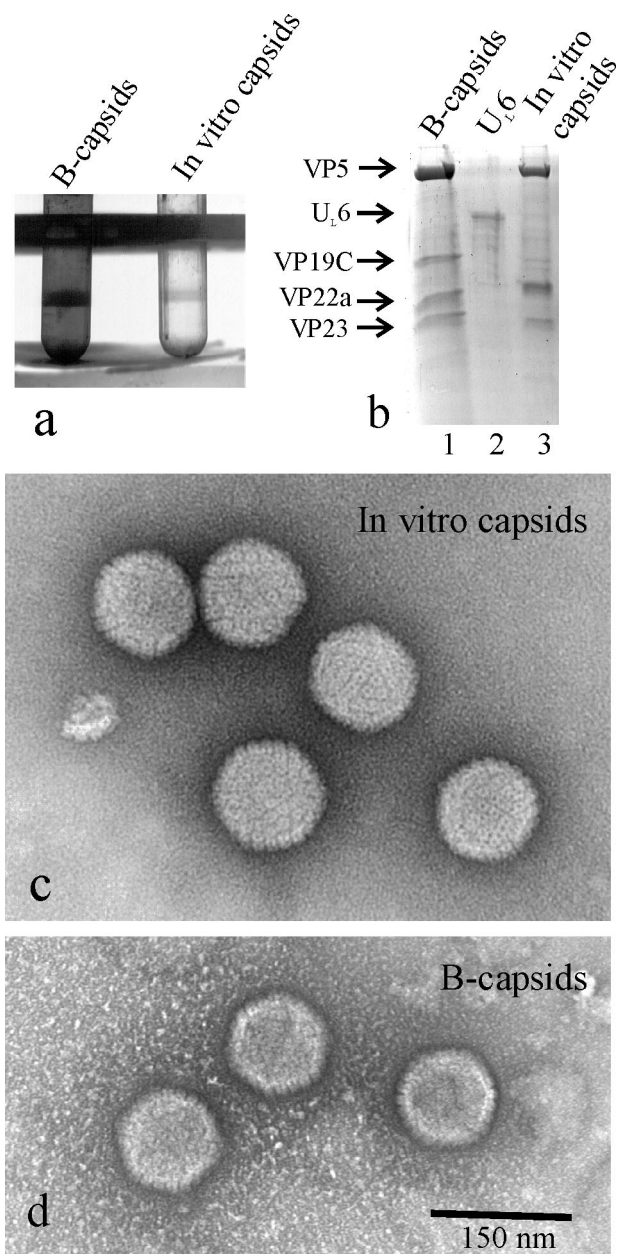


FIG. 6. Characterization of capsids formed in the in vitro capsid assembly system. Capsids assembled in vitro were compared to HSV-1 B capsids in sedimentation rate on sucrose density gradients (a), protein composition as determined by SDS-polyacrylamide gel electrophoresis followed by Coomassie staining (b), and electron microscopy (c and d). Note the similarity of capsids formed in vitro to B capsids in all three parameters.

32°C to allow capsids to form. The reaction mixtures were then centrifuged on a sucrose gradient to separate capsids from other reaction components. Examination of the gradients showed a single band of capsids that migrated at approximately the same rate as B capsids prepared from HSV-1-infected cells (Fig. 6a). Further experiments, described below, were carried out with capsids harvested from these gradients and concentrated by centrifugation into a pellet.

SDS-polyacrylamide gel analysis of the capsids showed that

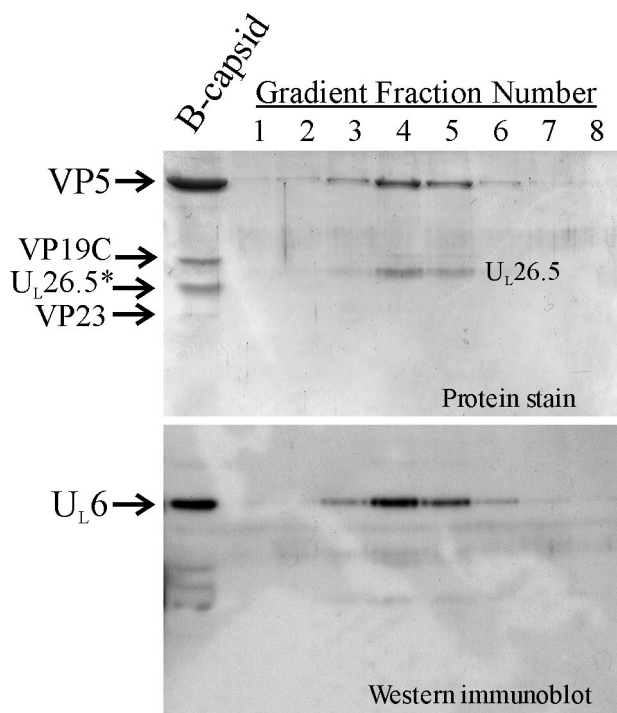


FIG. 7. U_L6 content of capsids formed in the in vitro capsid assembly system. The reaction mixtures contained scaffold-portal particles prepared from U_L26.5 and U_L6. Capsids were assembled in vitro and purified by two steps of sucrose density gradient centrifugation as described in Materials and Methods. After the second sucrose gradient step, capsid-containing fractions were analyzed by SDS-polyacrylamide gel electrophoresis followed by Coomassie staining (top) or immunoblot staining for U_L6 (bottom). Note that capsids contained U_L6.

they contained VP5, scaffolding protein (U_L26.5), and VP23 in the expected proportions (Fig. 6b, lane 3). The amount of VP19C was reduced compared to B capsids (compare Fig. 6b, lanes 1 and 3), an observation we attribute to proteolytic digestion occurring at the time the capsids were formed. Electron microscopic examination of the capsids after negative staining showed that they were uniform in size, with the diameter and angular morphology characteristic of mature capsids (Fig. 6c). Capsomers could be distinguished on the surfaces. Images of capsids formed in vitro were indistinguishable from those of B capsids isolated from infected cells (compare Figs. 6c and d).

Capsids formed in vitro were tested for the presence of U_L6 by SDS-polyacrylamide gel electrophoresis followed by specific Western blot staining. Experiments were performed with capsids that were purified by a second cycle of sucrose gradient centrifugation; capsid-containing and flanking fractions were analyzed.

The results showed that the capsid peak, as judged by the presence of VP5, coincided with a peak of U_L6 staining (Fig. 7). Only capsid-containing fractions were found to stain positively for U_L6. We interpret this result to indicate that U_L6 is associated with capsids.

The U_L6 copy number per capsid was determined quantitatively after densitometric scanning of the blot. As described in Materials and Methods, the integrated intensity of VP5 stain-

ing was taken as a measure of the total number of capsids present, while the immunoblot was used to determine the amount of U_L6. The U_L6/VP5 ratio observed in B capsids (leftmost lane in Fig. 7) was assumed to be 12 and used to scale the same ratios measured for capsids assembled in vitro. When measured in this way, values of 16.4 and 14.8 U_L6 molecules per capsid were obtained in two determinations.

Finally, an experiment was carried out to test whether the portal was stably associated with capsids formed in vitro. In such capsids, the portal could be firmly attached at a capsid vertex as it is in the native HSV-1 capsid, but it could also be less specifically attached, for example, as a part of the scaffold mass inside the shell or attached nonspecifically to the exterior of the capsid.

Tests were carried out by extracting capsids with 2.0 M GuHCl, a treatment that removes the scaffold from the capsid cavity and the pentons plus some triplexes from the shell (28). Most U_L6 remains, however, when extractions are performed with B capsids isolated from HSV-1-infected cells or with B capsids isolated from insect cells multiply infected with rBV encoding capsid proteins (18).

Capsids to be extracted were formed in vitro in reaction mixtures containing scaffold-portal particles plus VP5, triplexes, and U_L26/61. Capsids were isolated by sucrose gradient centrifugation, treated with 2.0 M GuHCl (or control buffer), and reisolated by sucrose gradient centrifugation. Capsid-containing fractions were then analyzed by SDS-polyacrylamide gel electrophoresis followed by protein staining for VP5 and Western immunostaining for U_L6. The results showed that U_L6 was present in capsids both before and after GuHCl treatment (Fig. 8, compare lanes 7 to 9 with lanes 10 to 12). Similar treatment of B capsids isolated from infected cells also failed to remove all the U_L6 (Fig. 8, compare lanes 1 to 3 with lanes 4 to 6). Quantitative measurements showed that the amounts of U_L6 remaining were 56 and 51%, respectively, after GuHCl treatment of B capsids assembled in vitro and control B capsids (Table 1).

DISCUSSION

Location of the HSV-1 portal at a unique vertex requires that capsid assembly occur in such a way that a single portal is incorporated into the growing structure while others are prevented from being incorporated. Three possible assembly mechanisms suggest themselves. (i) Procapsid assembly could be initiated by the portal or the portal in conjunction with other capsid proteins. Because initiation is a singular event in the assembly process, involvement of the portal could explain its unique location. (ii) The portal could be incorporated at an intermediate stage of assembly, provided there is a mechanism to insure that no additional portals can be added. (iii) Portal incorporation could be the final step in procapsid formation, assuring its singularity because there are no further additions to the structure.

Portal incorporation during capsid assembly has been examined in double-stranded DNA bacteriophages, which resemble herpesviruses in having a portal located at a unique capsid vertex. Considering experimental results with phages T4 and λ , Kochan et al. and Murialdo and Becker suggested that the portal might be involved in initiation of procapsid formation

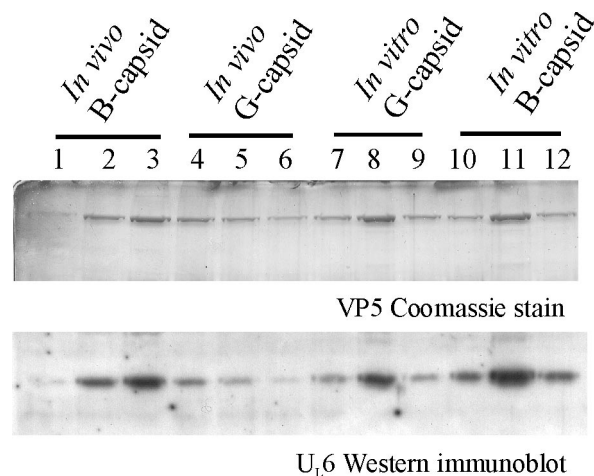


FIG. 8. Effects of GuHCl on the U_L6 contents of capsids isolated from infected cells (in vivo capsids) and capsids formed in the in vitro assembly system (in vitro capsids). Procedures described in Materials and Methods were used for isolating capsids by sucrose density gradient centrifugation, treating capsids in vitro with 2.0 M GuHCl, and reisolating them by sucrose gradient centrifugation. Capsid-containing fractions were then analyzed by SDS-polyacrylamide gel electrophoresis followed by Coomassie staining (top) or immunoblot staining for U_L6 (bottom). Untreated and treated capsids are called B capsids and G capsids, respectively. Note that U_L6 was resistant to extraction with 2.0 M GuHCl in capsids formed in vivo and in vitro. Since the number of capsids was different in each of the four specimens, quantitative determination of the amount of U_L6 present required that the U_L6 signal be scaled to that of VP5. The results of the quantitative analysis are shown in Table 1.

(13, 21). For instance, pertinent analyses were carried out with *Escherichia coli* after infection with a portal-negative mutant of phage T4 (gp20⁻). In such infections, capsid formation was found to be delayed compared to the wild-type (wt) virus, suggesting a role for gp20 in initiation (14). Capsid morphology is drastically affected in gp20⁻-infected cells. During infection with wt T4, incomplete capsid shells are found to be associated with portal-containing cores. This observation was interpreted to indicate that capsid assembly proceeds by initiation with a portal-scaffolding protein complex (the core), followed by formation of the capsid shell around the core (45, 46).

Results with HSV-1 and with phages ϕ 29 and P22 are more

TABLE 1. U_L6 copy numbers in control HSV-1 capsids and in capsids treated with 2.0 M GuHCl^a

Capsid type	GuHCl treatment	U _L 6 copy no.	U _L 6 remaining after GuHCl treatment (%)
In vivo B capsid	No	≡12.0	100
In vivo B capsid	Yes	6.1	51
In vitro B capsid	No	14.8	100
In vitro B capsid	Yes	8.3	56

^a U_L6 copy numbers were calculated after densitometric scanning of the gel electrophoresis results shown in Fig. 8. Coomassie staining of VP5 was determined as an overall measure of the number of capsids present, and the value was used to scale the amount of U_L6 as determined by Western immunoblotting. The VP5 (Coomassie)/U_L6 (Western) ratio determined for untreated B capsids isolated from infected cells (in vivo B capsids) was assumed to correspond to a U_L6 copy number of 12. For each capsid type, measurements were made with the gradient fraction having the highest level of VP5 staining, fractions 3, 4, 8, and 11 (Fig. 8).

difficult to interpret. In all three cases, the capsid shell and scaffolding proteins can form closed capsids in the absence of the portal protein (8, 24, 31, 32, 40, 42). Such portal-negative capsids can be formed both *in vivo* and *in vitro*. In fact, in a particularly revealing study with phage P22, it was demonstrated that incorporation of the portal did not greatly affect the rate of capsid formation *in vivo* (2). Such observations demonstrate that capsid formation can be initiated and completed without participation of the portal. As the portal is not required for initiation of capsid assembly, it is suggested that portal incorporation may occur after the initiation step. However, the above observations also raise questions regarding whether assembly of portal-containing capsids can be initiated by something other than the portal and how assembly of portal-negative capsids is avoided in cells infected with wt virus.

Scaffold-portal interaction. Interaction between the scaffolding and portal proteins has been demonstrated in studies carried out with phages T4, ϕ 29, and P22. In the case of T4, for example, the scaffold and portal proteins are suggested to interact because both are present in the cores involved in initiation of procapsid assembly, as described above (45, 46). Purified ϕ 29 scaffolding and portal proteins were found to interact after being mixed *in vitro*; Lee and Guo used sucrose gradient centrifugation to isolate complexes of the two proteins (15). Lastly, an interaction with the portal protein was suggested by analysis of certain P22 scaffolding protein mutants. Assembly of the portal into the capsid was found to be defective in two such mutants, which was interpreted to identify a scaffold site involved in contact with the portal (7).

Evidence is provided here for an interaction between the HSV-1 portal and the scaffolding protein. Complexes containing the two were formed after the purified components were mixed *in vitro*, and the complexes were found to be stable during isolation. Electron microscopic analysis of the complexes prepared by sucrose gradient centrifugation showed that they resemble the 55-nm-diameter scaffold particles formed from $U_L26.5$. They differed, however, in that one or more intact portals were observed on the surfaces of the scaffold-portal particles (Fig. 3, bottom). Compared to scaffold particles, scaffold-portal particles were found to be slightly larger in size and more heterogeneous in structure, suggesting that binding of the portal caused them to expand somewhat or perhaps to respond differently to the staining procedure employed (Fig. 3 and 4).

During agarose gel electrophoresis, scaffold-portal particles were found to migrate as a single species that contained both $U_L26.5$ and U_L6 ; the mobility of this species during electrophoresis was nearly the same as that of scaffold particles (Fig. 1a). Since the $U_L26.5$ - U_L6 complex was the major species observed by Ponceau S staining of the gel, it is suggested that it corresponds to the scaffold-portal particles isolated by sucrose gradient centrifugation and observed by electron microscopy.

The use of SDS-polyacrylamide gel electrophoresis to measure the protein composition of scaffold-portal particles revealed that portals combine in various proportions with scaffold particles. The largest amount of U_L6 that we observed bound to $U_L26.5$ corresponded to a molar ratio of ~ 14 $U_L26.5$:1 U_L6 (Fig. 2). This ratio can be interpreted in terms of scaffold-particle structure if we note that the scaffold particle

mass, as determined by McClelland et al. (14.7 to 18.4 MDa) ([17]) corresponds to a range of 435 to 545 $U_L26.5$ molecules (MW, 33,760) per scaffold particle. Using this range of values, the maximum U_L6 binding can be calculated to correspond to a range of ~ 30 to 38 U_L6 molecules, or two or three portals, per scaffold particle. This relatively low number of portals bound to each scaffold particle (i.e., two or three portals for several hundred $U_L26.5$ molecules) indicates that not all scaffold molecules are capable of binding a portal. We suggest that binding-competent $U_L26.5$ molecules may differ from others in conformational state or in the region displayed on the scaffold particle surface.

WAY-150138. WAY-150138 is a member of a novel class of thiourea compounds able to inhibit HSV-1 replication in cell culture (23, 47); a similar compound affects the replication of varicella-zoster virus (48). Studies designed to clarify the mechanism of WAY-150138 action suggest that it functions by inhibiting encapsidation of viral DNA. When cells are infected with HSV-1 in the presence of the drug, progeny capsids form normally, but they lack DNA (47). WAY-150138-resistant mutants are found to map to the U_L6 gene, indicating a possible effect of the drug on the portal. Further clarification of the mechanism of WAY-150138 action was obtained in biochemical analyses of the capsids formed in the presence of the drug. Such capsids were found to be depleted in the portal, suggesting that WAY-150138 acts by depriving capsids of the portal during the assembly process (23).

We reasoned that the effects of WAY-150138 on virus replication would be explained if the drug antagonizes the interaction between the portal and the scaffolding protein. Provided that incorporation of a portal into the growing capsid proceeds by way of a scaffold-portal complex, then prevention of complex formation should lead to assembly of capsids lacking the portal. To test this idea, we examined the effect of the drug on the formation of scaffold-portal complexes *in vitro*. The results (Fig. 5) demonstrated inhibition over a range of drug concentrations found to be effective in attenuating HSV-1 replication (47). WAY-150138 inhibited complex formation without producing a dramatic effect on scaffold particle structure, as judged by particle mobility during agarose gel electrophoresis (Fig. 5a and b). Inhibition of complex formation *in vitro* supports the view that WAY-150138 affects HSV-1 replication by antagonizing the interaction between the portal and the scaffolding protein.

In vitro capsid assembly. An *in vitro* capsid assembly system was employed to test the ability of scaffold-portal particles to function in the formation of portal-containing capsids. In addition to scaffold-portal particles, the system contained the major capsid protein, triplexes, and the maturational protease. To our knowledge, this is the first report of an *in vitro* system in which portal-containing capsids are formed. Capsids assembled in the system were found to have the structure and protein composition of the mature capsid (Fig. 6), and U_L6 was demonstrated by Western immunoblot analyses to be present in the capsids (Fig. 7). The measured level of U_L6 (16.4 and 14.8 molecules per capsid in two experiments) was in satisfactory agreement with the value of 12 expected if each capsid has a single portal. We suggest that the slightly higher measured values (i.e., 16.4 and 14.8) may result from the fact that a small

number of capsomers are often found to be missing in capsids assembled *in vitro*.

A control experiment was carried out to address the issue of whether the portals assembled into capsids in the *in vitro* system are associated with the capsid shell in the same way they are in capsids formed in infected cells. Capsids were extracted *in vitro* with 2.0 M GuHCl, and the amount of U_L6 remaining was determined by Western blot analysis. The results showed that the amounts of U_L6 extracted from *in vitro* and *in vivo* capsids were very similar: ~50% was extracted in both cases. We interpret this result to suggest that portal binding to the capsid shell is the same in the two capsid types (Fig. 8 and Table 1).

The ability of scaffold-portal particles to participate in the formation of portal-containing capsids *in vitro*, as reported here, supports the view that similar scaffold-portal complexes may be involved in capsid assembly *in vivo*. Assembly of the portal into the capsid by way of a complex with the scaffolding protein is consistent with the results, mentioned above, demonstrating that certain scaffolding protein mutants of phage P22 are defective in incorporation of the portal into capsids (7). Such mutations are expected if scaffold-portal complexes are involved in assembly of the portal into capsids.

It is also interesting to note that U_L6 appears to be present in scaffold-portal particles in the form of intact portals rather than smaller oligomers or monomers. In fact, assembled portals are the smallest oligomeric state we have observed for U_L6 *in vitro* (W. Newcomb and J. Brown, unpublished observations). U_L6 contrasts in this respect with the P22 portal protein (gp1), in which monomers and other oligomers are observed (1, 19, 20). The presence of intact portals in scaffold-portal particles is most consistent with the view that U_L6 is incorporated into the nascent capsid as a preformed, intact dodecamer. We note that assembly of preformed structures is a familiar theme arising from studies of the morphogenesis of T4 and other bacteriophages (4).

The formulation of an *in vitro* system for the assembly of portal-containing capsids, as reported here, encourages the hope that future studies may help resolve the issue of how capsids are formed with a single portal. The ability to manipulate the protein composition and other variables of *in vitro* reaction mixtures provides a versatility of experimental design that may provide clues about this intriguing problem.

ACKNOWLEDGMENTS

We thank Marja van Zeijl (Wyeth Research) for a generous gift of WAY-150138.

This work was supported by grants from the National Institutes of Health (AI41644), the National Science Foundation (MCB-9904879), and the Virginia Commonwealth Health Research Board (GN 01-10).

REFERENCES

- Bazinet, C., J. Benbasat, J. King, J. M. Carazo, and J. L. Carrascosa. 1988. Purification and organization of the gene 1 portal protein required for phage P22 DNA packaging. *Biochemistry* **27**:1849–1856.
- Bazinet, C., and J. King. 1988. Initiation of P22 procapsid assembly *in vivo*. *J. Mol. Biol.* **202**:77–86.
- Brown, J. C., M. A. McVoy, and F. L. Homa. 2001. Packaging DNA into herpesvirus capsids, p. 111–153. *In* A. Holzenburg and E. Bogner (ed.), *Structure-function relationships of human pathogenic viruses*. Kluwer Academic Publishers, London, United Kingdom.
- Eiserling, F. A., and L. W. Black. 1994. Pathways in T4 morphogenesis, p. 209–212. *In* J. D. Karam (ed.), *Molecular biology of bacteriophage T4*. ASM Press, Washington, D.C.
- Engvall, E., and P. Perlman. 1971. Enzyme-linked immunosorbent assay (ELISA): quantitative assay for immunoglobulin. *Immunochemistry* **8**:871–874.
- Ey, P. L., S. J. Prowse, and C. R. Jenkin. 1978. Isolation of pure IgG₁, IgG_{2a} and IgG_{2b} immunoglobulins from mouse serum using protein A-sepharose. *Immunochemistry* **15**:429–436.
- Greene, B., and J. King. 1996. Scaffolding mutants identifying domains required for P22 procapsid assembly and maturation. *Virology* **225**:82–96.
- Guo, P., S. Erickson, W. Xu, N. Olson, T. S. Baker, and D. Anderson. 1991. Regulation of the phage phi 29 prohead shape and size by the portal vertex. *Virology* **183**:366–373.
- Heymann, J. B., N. Cheng, W. W. Newcomb, B. L. Trus, J. C. Brown, and A. C. Steven. 2003. Dynamics of herpes simplex virus capsid maturation visualized by time-lapse cryo-electron microscopy. *Nat. Struct. Biol.* **10**:334–341.
- Homa, F. L., and J. C. Brown. 1997. Capsid assembly and DNA packaging in herpes simplex virus. *Rev. Med. Virol.* **7**:107–122.
- Hong, Z., M. Beaudet-Miller, J. Durkin, R. Zhang, and A. D. Kwong. 1996. Identification of a minimal hydrophobic domain in the herpes simplex virus type 1 scaffolding protein which is required for interaction with the major capsid protein. *J. Virol.* **70**:533–540.
- Kennard, J., F. J. Rixon, I. M. McDougall, J. D. Tatman, and V. G. Preston. 1995. The 25 amino acid residues at the carboxyl terminus of the herpes simplex virus type 1 UL26.5 protein are required for the formation of the capsid shell around the scaffold. *J. Gen. Virol.* **76**:1611–1621.
- Kochan, J., J. L. Carrascosa, and H. Murialdo. 1984. Bacteriophage lambda preconnectors. Purification and structure. *J. Mol. Biol.* **174**:433–447.
- Laemmli, U. K., and F. A. Eiserling. 1968. Studies on the morphogenesis of the head of phage T-even. V. The formation of polyheads. *Mol. Gen. Genet.* **101**:333–345.
- Lee, C. S., and P. Guo. 1995. Sequential interactions of structural proteins in phage phi 29 procapsid assembly. *J. Virol.* **69**:5024–5032.
- Matusick-Kumar, L., W. W. Newcomb, J. C. Brown, P. J. McCann, W. Hurlburt, S. P. Weinheimer, and M. Gao. 1995. The C-terminal 25 amino acids of the protease and its substrate ICP35 of herpes simplex virus type 1 are involved in formation of sealed capsids. *J. Virol.* **69**:4347–4356.
- McClelland, D. A., J. D. Aitken, D. Bhella, D. McNab, J. Mitchell, S. M. Kelly, N. C. Price, and F. J. Rixon. 2002. pH reduction as a trigger for dissociation of herpes simplex virus type 1 scaffolds. *J. Virol.* **76**:7407–7417.
- McNab, A. R., P. Desai, S. Person, L. L. Roof, D. R. Thomsen, W. W. Newcomb, J. C. Brown, and F. L. Homa. 1998. The product of the herpes simplex virus type 1 UL25 gene is required for encapsidation but not for cleavage of replicated viral DNA. *J. Virol.* **72**:1060–1070.
- Moore, S. D., and P. E. Prevelige, Jr. 2001. Structural transformations accompanying the assembly of bacteriophage P22 portal protein rings *in vitro*. *J. Biol. Chem.* **276**:6779–6788.
- Moore, S. D., and P. E. Prevelige, Jr. 2002. Bacteriophage p22 portal vertex formation *in vivo*. *J. Mol. Biol.* **315**:975–994.
- Murialdo, H., and A. Becker. 1978. Head morphogenesis of complex double-stranded deoxyribonucleic acid bacteriophages. *Microbiol. Rev.* **42**:529–576.
- Newcomb, W. W., and J. C. Brown. 1989. Use of Ar⁺ plasma etching to localize structural proteins in the capsid of herpes simplex virus type 1. *J. Virol.* **63**:4697–4702.
- Newcomb, W. W., and J. C. Brown. 2002. Inhibition of herpes simplex virus replication by WAY-150138: assembly of capsids depleted of the portal and terminase proteins involved in DNA encapsidation. *J. Virol.* **76**:10084–10088.
- Newcomb, W. W., F. L. Homa, D. R. Thomsen, F. P. Booy, B. L. Trus, A. C. Steven, J. V. Spencer, and J. C. Brown. 1996. Assembly of the herpes simplex virus capsid: characterization of intermediates observed during cell-free capsid assembly. *J. Mol. Biol.* **263**:432–446.
- Newcomb, W. W., F. L. Homa, D. R. Thomsen, B. L. Trus, N. Cheng, A. C. Steven, F. P. Booy, and J. C. Brown. 1999. Assembly of the herpes simplex virus procapsid from purified components and identification of small complexes containing the major capsid and scaffolding proteins. *J. Virol.* **73**:4239–4250.
- Newcomb, W. W., F. L. Homa, D. R. Thomsen, Z. Ye, and J. C. Brown. 1994. Cell-free assembly of the herpes simplex virus capsid. *J. Virol.* **68**:6059–6063.
- Newcomb, W. W., R. M. Juhas, D. R. Thomsen, F. L. Homa, A. D. Burch, S. K. Weller, and J. C. Brown. 2001. The UL6 gene product forms the portal for entry of DNA into the herpes simplex virus capsid. *J. Virol.* **75**:10923–10932.
- Newcomb, W. W., B. L. Trus, F. P. Booy, A. C. Steven, J. S. Wall, and J. C. Brown. 1993. Structure of the herpes simplex virus capsid: molecular composition of the pentons and the triplexes. *J. Mol. Biol.* **232**:499–511.
- Newcomb, W. W., B. L. Trus, N. Cheng, A. C. Steven, A. K. Sheaffer, D. J. Tenney, S. K. Weller, and J. C. Brown. 2000. Isolation of herpes simplex virus procapsids from cells infected with a protease-deficient mutant virus. *J. Virol.* **74**:1663–1673.
- Orlova, E. V., P. Dube, E. Beckmann, F. Zemlin, R. Lurz, T. A. Trautner, P. Tavares, and M. van Heel. 1999. Structure of the 13-fold symmetric portal protein of bacteriophage SPPI. *Nat. Struct. Biol.* **6**:842–846.

31. **Patel, A. H., F. J. Rixon, C. Cunningham, and A. J. Davison.** 1996. Isolation and characterization of a herpes simplex virus type-1 mutant defective in the UL6 gene. *Virology* **217**:111–123.
32. **Prevelige, P. E., D. Thomas, and J. King.** 1993. Nucleation and growth phases in the polymerization of coat and scaffolding subunits into icosahedral procapsid shells. *Biophys. J.* **64**:824–835.
33. **Rixon, F. J.** 1993. Structure and assembly of herpesviruses. *Semin. Virol.* **4**:135–144.
34. **Roizman, B., and A. E. Sears.** 1996. Herpes simplex viruses and their replication, p. 2231–2295. *In* B. N. Fields, D. M. Knipe, P. M. Howley, R. M. Chanock, J. L. Melnick, T. P. Monath, B. Roizman, and S. E. Straus (ed.), *Fields virology*. Lippincott-Raven, Philadelphia, Pa.
35. **Shulman, M., C. D. Wilde, and G. Kohler.** 1978. A better cell line for making hybridomas secreting specific antibodies. *Nature* **276**:269–270.
36. **Simpson, A. A., Y. Tao, P. G. Leiman, M. O. Badasso, Y. He, P. J. Jardine, N. H. Olson, M. C. Morais, S. Grimes, D. L. Anderson, T. S. Baker, and M. G. Rossmann.** 2000. Structure of the bacteriophage phi29 DNA packaging motor. *Nature* **408**:745–750.
37. **Smith, D. E., S. J. Tans, S. B. Smith, S. Grimes, D. L. Anderson, and C. Bustamante.** 2001. The bacteriophage straight phi29 portal motor can package DNA against a large internal force. *Nature* **413**:748–752.
38. **Steven, A. C., and P. G. Spear.** 1996. Herpesvirus capsid assembly and envelopment, p. 312–351. *In* R. Burnett, W. Chiu, and R. Garcea (ed.), *Structural biology of viruses*. Oxford University Press, New York, N.Y.
39. **Tao, Y., N. H. Olson, W. Xu, D. L. Anderson, M. G. Rossmann, and T. S. Baker.** 1998. Assembly of a tailed bacterial virus and its genome release studied in three dimensions. *Cell* **95**:431–437.
40. **Tatman, J. D., V. G. Preston, P. Nicholson, R. M. Elliott, and F. J. Rixon.** 1994. Assembly of herpes simplex virus type 1 capsids using a panel of recombinant baculoviruses. *J. Gen. Virol.* **75**:1101–1113.
41. **Thomsen, D. R., W. W. Newcomb, J. C. Brown, and F. L. Homa.** 1995. Assembly of the herpes simplex virus capsid: requirement for the carboxyl-terminal 25 amino acids of the proteins encoded by the UL26 and UL26.5 genes. *J. Virol.* **69**:3690–3703.
42. **Thomsen, D. R., L. L. Roof, and F. L. Homa.** 1994. Assembly of herpes simplex virus (HSV) intermediate capsids in insect cells infected with recombinant baculoviruses expressing HSV capsid proteins. *J. Virol.* **68**:2442–2457.
43. **Trus, B. L., F. P. Booy, W. W. Newcomb, J. C. Brown, F. L. Homa, D. R. Thomsen, and A. C. Steven.** 1996. The herpes simplex virus procapsid: structure, conformational changes upon maturation, and roles of the triplex proteins VP19C and VP23 in assembly. *J. Mol. Biol.* **263**:447–462.
44. **Trus, B. L., F. L. Homa, F. P. Booy, W. W. Newcomb, D. R. Thomsen, N. Cheng, J. C. Brown, and A. C. Steven.** 1995. Herpes simplex virus capsids assembled in insect cells infected with recombinant baculoviruses: structural authenticity and localization of VP26. *J. Virol.* **69**:7362–7366.
45. **van Driel, R., and E. Couture.** 1978. Assembly of bacteriophage T4 head-related structures. II. In vitro assembly of prehead-like structures. *J. Mol. Biol.* **123**:115–128.
46. **van Driel, R., and E. Couture.** 1978. Assembly of the scaffolding core of bacteriophage T4 proheads. *J. Mol. Biol.* **123**:713–719.
47. **van Zeijl, M., J. Fairhurst, T. R. Jones, S. K. Vernon, J. Morin, J. LaRocque, B. Feld, B. O'Hara, J. D. Bloom, and S. V. Johann.** 2000. Novel class of thiourea compounds that inhibit herpes simplex virus type 1 DNA cleavage and encapsidation: resistance maps to the UL6 gene. *J. Virol.* **74**:9054–9061.
48. **Visalli, R. J., J. Fairhurst, S. Srinivas, W. Hu, B. Feld, M. DiGrandi, K. Curran, A. Ross, J. D. Bloom, M. van Zeijl, T. R. Jones, J. O'Connell, and J. I. Cohen.** 2003. Identification of small molecule compounds that selectively inhibit varicella-zoster virus replication. *J. Virol.* **77**:2349–2358.
49. **Zhou, Z. H., M. Dougherty, J. Jakana, J. He, F. J. Rixon, and W. Chiu.** 2000. Seeing the herpesvirus capsid at 8.5 Å. *Science* **288**:877–880.